The Effect of Adhesive Failure and Defects on the Stress Distribution in All-ceramic Crowns

Yonggang Liu[1], Yuanzhi Xu[2], Bo Su[3], Dwayne Arola[4,5,6], *Dongsheng Zhang[6,7]

[1]Shanghai Institute of Applied Mathematics and Mechanics,

Shanghai, 200072, PR China

[2]The Tenth People's Hospital of Tongji University

Shanghai, 200072, PR China

[3]Bristol Dental School, University of Bristol, Bristol, BS1 2LY, UK

[4]Department of Materials Science and Engineering, University of Washington, Seattle, WA,

USA 98195

[5]Department of Restorative Dentistry, School of Dentistry, University of Washington, Seattle, WA USA 98195

[6]Department of Mechanics, Shanghai University, Shanghai, 200444, China

[7]Shanghai Key Laboratory of Mechanics in Energy Engineering,

Shanghai, 200072, China

*Corresponding author:
Dongsheng Zhang, Ph.D.
Department of Mechanics
Shanghai University
99 Shangda Road, Shanghai, 200444 PR China
donzhang@staff.shu.edu.cn
Tel.:0086-21-6613-5258

ABSTRACT

Objectives: To explore the effect of adhesive failure and defects between the crown and cement on the stress distribution within all-ceramic crowns and the corresponding risk of failure.

Methods: An IPS e.max crown of lithium disilicate produced by CAD/CAM for a first mandibular molar was modeled using finite element analysis based on X-ray micro-CT scanned images. Predefined debonding states and interfacial defects between the crown and cement were simulated using the model. The first principal stress distribution of the crown and cement was analyzed under a vertical occlusal load of 600 N. A concept of failure risk was proposed to evaluate the crown.

Results: Stress concentrations in the crown were identified on the occlusal surface surrounding the region of loading, beneath the area of loading and at the margin of the interior surface. Stress concentrations in the cement were also evident at the boundary of the debonded areas. The lower surface of the crown is safe to sustain the 600 N vertical load, but the top surface of the cement would undergo cohesive failure. According to the evaluation of failure risk of the crown, the conditions of highest risk corresponded to the conditions with highest percentage of cement damage. The risk of failure is not only associated with debonding between the crown and cement, but also associated with its distribution.

Conclusions: Debonding related defects and cementing defects are more deleterious to the interfacial stress than debonding itself. The axial wall plays a critical role in maintaining the principal tensile stress of the crown at an acceptable level.

Clinical Significance: Interfacial defects between the crown and cement are more deleterious than debonding itself to crown failures. Processes should be developed to minimize these defects during the placement of crowns as much as possible.

Keywords: Ceramic crown; Debonding; Defects; Failure risk; Finite Element Analysis (FEA) ; Lithium disilicate

1. Introduction

All-ceramic crowns have quickly become commonplace in clinical practice due to a combination of desirable properties, such as aesthetics, biocompatibility and durability [1]. But due to their brittle behavior, all-ceramic crowns are more likely to fracture than their predecessors (e.g. metal or porcelain-fused-to-metal crowns) when they are used as dental prostheses [2, 3]. In general, posterior all-ceramic restorations are subjected to much larger forces than those in the anterior region and this leads to a higher rate of failure [3].

Based on the higher relative risk of fracture of all-ceramic restorations, substantial efforts have been made to address this problem over the past two decades. The introduction of Computer Aided Design/Computer Aided Manufacturing (CAD/CAM) has helped to fabricate all-ceramic crowns with improved quality, minimizing drawbacks like voids and other volumetric defects. CAD/CAM also offers dentists the opportunity to prepare, design and fabricate ceramic restorations in a single appointment [4, 5]. The inherent fracture strength of dental ceramic materials has been improved as well. For instance, the strength of zirconia, a core ceramic in double layered crown restorations, has reportedly exceeded 900 MPa [6-8].

Lithium disilicate glass-ceramic exhibits excellent shade varieties and translucency. Consequently, it has become an important veneer material for double-layer ceramic crowns [9, 10]. The newly developed CAD/CAM lithium disilicates possess a flexural strength of approximately 360 MPa, which is sufficient to be used for posterior monolithic restorations [11, 12]. Guess et al. [13] reported that IPS e.max CAD molar crowns were able to withstand masticatory forces. The reliability of monolithic lithium disilicate crowns has also been

confirmed by fatigue tests [13, 14]. Of course, a monolithic crown structure is advantageous as it eliminates the potential for failure associated with porcelain layering [15]. However, the load bearing capacity of ceramic crowns can be influenced by many factors, such as the tooth preparation, processes involved in manufacturing the restoration, and the luting process [16].

During the processes of manufacturing the restorations, several factors have been identified that may contribute to all-ceramic crown failures including [17]: (i) defects [18], (ii) residual stresses [19], and (iii) thermal residual stresses [20]. However, defects have been suggested to be the leading cause of failure [21]. Defects such as pores, inclusion and small cracks may cause stress concentration and become the site of subcritical crack growth [17]. Meanwhile, the fabrication of glass-ceramics may introduce processing defects, and crown failures are influenced by the size and location of such defects [22, 23]. Thus, it is worthwhile to explore the relationship between defects and the risk of crown failures [17].

In regards to the luting process, most contemporary dental adhesives are able to achieve acceptable immediate bond strength. However, the bond reliability is dependent on both physical and chemical effects [24]. Physical bonding effects include, for example, micromechanical interlocking of the resin with the porcelain surface, which would be enhanced by pre-cementation surface roughening through hydrofluoric acid etching [25] or air abrasion [26]. Chemical bonding effects may include utilizing silane coatings (bifunctional coupling agents), which mediate covalent bonding between the inorganic porcelain and the organic resin [27]. Pre-cementation surface roughening and silane application can enhance porcelain-resin adhesion, the immediate bond quality between ceramic and cement and the fracture resistance of ceramic crowns [28]. However, the

durability is a necessary consideration since bond degradation occurs via water sorption, hydrolysis of ester linkages of methacrylate resins, and activation of endogenous dentin matrix metalloproteinases [29].

The fracture resistance of all-ceramic restorations is maximized by improving the bond strength at the interface [30, 31]. However, according to an evaluation of clinically failed and retrieved all-ceramic crowns, over 90% of glass-ceramic restoration failures are related to defects and stresses at the bonded interface [32]. Adhesive failure and interfacial defects are clinically relevant and potentially contributing factors to crown fractures. Cracks and debonding at the cement interfaces may be induced by poor luting processes or degradation of the adhesion [33]. Furthermore, the bond strength between the ceramic and cement is greatly influenced by cement type and cement aging [34]. Degradation of the bond strength reduces the load bearing capacity of full-coverage restorations [35-37]. Besides, weak bonds generated by compromised adaptation may cause gaps and microleakage [38]. Secondary caries in the mouth may also cause adhesive failure between the crown and cement [39], or between the dentin and cement [5].

Hernandez et al. [39] reported that approximately 65% of failures of ceramic blocks bonded using resin cement to a flat dentin substrate were found debonded between ceramic and cement under conditions of either water storage or mechanical loading. Interestingly, Nasrin et al. [15] found that lithium disilicate crowns subjected to fatigue loading were more likely to undergo early debonding at the wall area near the margin. Debonding is believed to originate at the margin of the shoulder due to the existence of marginal gaps [31, 36]. These failures progress to the occlusal region with fatigue crack growth.

In general, simulating the process of adhesive failure that progresses over a long period of time is difficult to assess experimentally. The stress distribution within the cement that may contribute to interface failure is not available from experimental methods. Therefore, a numerical approach was adopted in this study to evaluate the stress distribution at the bonded interface between all-ceramic crown and tooth abutment with bonded interface debonding and defects. The aim of the present paper is to evaluate the risk of restored crown failure related to debonding and defects at the interface between the crown and cement. To understand the effect caused by interface debonding and its extent, a strategy of investigation was adopted that considered debonding percentages between crown and cement and different defect patterns. The null hypothesis of this investigation is that defects at the bonded interfaces do not increase the risk of all-ceramic crown failure.

2. Materials and Methods

2.1 Crown preparation

The monolithic lithium disilicate crown was selected as the ceramic restoration. The specific crown modeled in this investigation was based on IPS e.max CAD (Ivoclar Vivadent, Liechtenstein). A plaster mold and a concave silicon rubber mold were duplicated from the standard Asian first right mandibular molar (D50-500A, Nissin Dental Products Co., Ltd.). The crown of the duplicate was trimmed so that the occlusal reduction was about 2 mm at the contact area, and with coronal length of 4 mm; the shoulder was prepared with 1 mm reduction on the lingual and buccal surfaces. Lithium disilicate crowns require a minimum occlusal layer thickness of 1.5 - 2 mm to resist failure by cyclic loading in the mouth [40-42].

The trimmed tooth was tapered at 8 degrees with a 1 mm shoulder of 90º. Then the trimmed plaster mold was used to duplicate the dental substrate with Z100™ (3M ESPE, St. Paul, MI, USA). Instead of manufacturing the crown using IPS e.max CAD, the monolithic crown was prepared with a unique mixture of barium sulfate and denture base resin (Type II) (Shanghai Medical Instruments Co., Ltd., Shanghai, China) to develop high-contrast grayscale levels in X-ray radiation. The ratio of the two parts was 3:10 and the crown was built after the hardening process. The crown was carefully sanded and polished. The average thickness of the facet area of the crown was about 2 mm and the thickness gradually decreased to 1 mm at the shoulder.

2.2 Finite element modeling and simulation

The restored tooth was scanned with a GE micro-CT scanner with a voxel resolution of 20 μm. The sequential sliced images were imported into the 3D image conversion software, Simpleware (version 6.0, Simpleware Ltd., UK), in Dicom format, which converted the sliced images acquired from CT into a numerical 3D model. The software also provided means for smoothing the surface, assigning material properties and meshing. As shown in Fig. 1, the meshed model contained three components including the ceramic crown, cement layer and tooth substrate. Some important geometric dimensions are included in the figure for reference. The meshed model was imported into ABAQUS/CAE 6.10 software (Dassault Systemes Simulia Corp., Providence, RI, USA). Details of the final meshed models and material parameters are listed in Table 1. Note that the restoration was cemented to the dentin substrate using RelyX ARC (3M-ESPE St. Paul, MN) in the simulation, which is common

practice in China. In the finite element analysis (FEA), all of the materials were treated as linear-elastic, isotropic, and homogeneous [45]. According to the microstructure, dentin is basically anisotropic. However, since the purpose of this study is to analyze the stress distribution in the ceramic crown, the substrate dentin was treated as an isotropic continuum with linear elastic properties [46]. In addition, since the inhomogeneity of the tubule is several orders of magnitude smaller than the features of the crown preparation, the substrate dentine was also regarded as homogeneous and a continuum.

In order to evaluate the stress distribution within the monolithic restoration and account for evolution of debonding, seven finite element (FE) models were generated. Due to the differences in geometry, these models had a different number of total elements and nodes. A convergence analysis was conducted for each model to avoid quantitative differences in the stress values associated with meshing.

According to Lu et al. [36], water sorption could facilitate debonding between the crown and tooth substrate at the shoulder and even at the early stage of loading. With increasing load, the likelihood and extent of debonding increased until the radial cracks initiated beneath occlusal region and eventually caused bulk fracture of the crown. Based on these experimental observations, a seven-stage debonding process was conceived to evaluate the redistribution in stress with the extension of debonding from the shoulder to central occlusal region, until complete debonding. This seven-stage model is depicted in Fig. 2(a) through 2(g) and corresponds to percentage of debonding that ranges from 0 to 100%. In Fig. 2, the shaded areas represent the debonded regions and the gray areas represent the regions that remain soundly bonded.

Defects distributed along the bonded interface have also been reported as a leading cause of crown failures [21]. The fabrication of glass-ceramics may introduce both intrinsic and processing defects [22, 23]. A previous study using micro-CT analysis showed that multiple pores ranging from 50 μm to 300 μm existed within the veneer and core of all-ceramic crowns [47]. Furthermore, Jian et al. [17] reported that the pores located at or next to the veneer–core interface in bilayered lithium disilicate glass-ceramics have diameters ranging from roughly 440 μm to 1180 μm. In the present study, only pores (intrinsic or introduced by acid etching or airborne alumina particle air abrasion) located at the interface between the crown and cement were considered. A defect pattern at the bonded interface was designed based on the literature [17, 47] (Fig. 2(h) and 2(i)). Of course, these are idealized defects and distribution. Although each defect has a unique geometry, a nominal diameter can be defined as the perimeter length of the defect divided by π. In this study, defects were assumed randomly distributed over the luting interface with average nominal diameters of 130 μm (Case I) and 500 μm (Case II). The percentages of the defect area over the luting interface were 2.6% and 13.3%, and the number density per 1 mm^2 is 2.85 and 1.10, respectively. These two cases are shown in Fig. 2(h) and 2(i).

Contact elements were defined in the areas of debonding (Fig. 2(a) through 2(g)), and the contact friction coefficient was set as 0.1 [45]. The remaining interface between the tooth substrate and cement was treated as perfectly bonded. Similarly, in Fig. 2(h) and 2(i), the shaded area represents defects at the luting surface. The contact boundary condition was applied with contact friction coefficient set as 0.1. The remaining interfaces were treated as perfectly bonded.

To calculate the stress distribution within the ceramic crown, the displacement components of nodes at the bottom of the model were constrained (Fig. 3). A 600 N [3, 48] vertical occlusal load was applied at the center of the restored crown via an analytical rigid hemisphere with diameter of 5 mm as shown in Fig. 3. The surface interaction between the hemisphere and crown was defined as smooth contact.

2.3 Evaluation of failure risk

In this study the average of the first principal stress, which was called as average stress, over the entire stressed body was used to facilitate the analysis concerning the risk of crown failures induced by cyclic stresses. The first principal stress at a point i in the stressed body can be defined as σ_i, and the ultimate tensile strength of this material is σ_u. The ratio $\eta_i = \sigma_i / \sigma_u$ was defined to describe the probability of fracture on a point of the monolithic crown subjected to cyclic loads.

Describing the material in a volumetric manner is one approach to account for the population and distribution of defects. In the finite element model of the monolithic crown, the total volume is V and contains N elements. In an arbitrary tiny element with volume V_i, the probability of fracture can also be evaluated with Eq. (1). By introducing the volume weight V_i / V, the total probability of fracture η can be modified using a weighted calculation by

For the lithium disilicate crown with ultimate tensile strength σ_u over the volume, Eq. (2) can be simplified as

where $\bar{\sigma}$ is the average stress mentioned above. Since the ultimate tensile strength σ_u is a constant, the average stress $\bar{\sigma}$ controls the level of probability of fracture of the lithium disilicate crown.

For brittle materials without cracks, the maximum tensile stress is used to establish whether the state of stress is safe. The Rankine criterion is useful to assess safety from the ratio $\lambda = \sigma_u / \sigma_{max}$, where locations with values greater than 1 are safe in the stressed body. The probability of fracture is inversely related to the ratio λ. Combining the two coefficients η and λ, the comprehensive risk of failure (κ) of the monolithic crown can be defined as follows:

The parameter κ reflects the risk of failure of the restored crown with considerations of the static effect λ and potential fatigue effect η. Since the term $\lambda = \sigma_u / \sigma_{max}$ represents safety reservation of the structure, and $\eta = \bar{\sigma} / \sigma_u$ represents the fracture probability per unit volume of the structure before crack, the ratio $\kappa = \eta / \lambda$ means the fracture probability per unit volume assigned per unit safety reservation.

3. Results

3.1 Stress distribution

The stress distributions at the seven-stage debonding processes corresponding to Stage 1 through Stage 7 are shown in Figs. 4(a) through 4(g), respectively, and the stress distribution corresponding to bonded interfaces with defects at the luting surface including Cases I and II are shown in Figs. 4(h) and 4(i), respectively. As evident from differences in the stress distributions, the debonding condition is important to the state of stress.

As evident from the principal stress distribution in Fig. 4(a), the stress at the internal surface of the ceramic crown is relatively uniform when the crown is completely bonded to the tooth substrate. The maximum tensile stress reached 59 MPa and appeared beneath one of the contact zones at the interior surface. The stress distribution varied with degree of debonding along the interior wall. A stress concentration develops at the debonding region, as evident in Figs. 4(b) and 4(c), and the magnitude of the tensile stress in this area increases. However, in the bonded occlusal region, the tensile stress at the interior surface remains approximately uniform. After the debonding expanded to the occlusal region, the magnitude of stress increased appreciably and a stress concentration is observed along the boundary of debonding (Figs. 4(d)-(f)). The maximum tensile stress in the monolithic crown reached nearly 100 MPa after complete separation between the restored crown and the cement (Fig. 4 (g)).

The stress distributions of the crown were also analyzed in terms of the distributed bonded interface defects. As shown in Figs. 4(h) and 4(i), the stress concentration was more distinct in the case of larger defects (Case II). Furthermore, the region of highest stress was

found in the occlusal region rather than the wall. It was interesting to note that the magnitude of stress caused by interfacial defects is greater than that caused by complete debonding.

The stress distributions in the cement caused by debonding and interfacial defects were also evaluated and results are presented in Fig. 5. Since the stress at the interface between the cement and substrate was less than that between the cement and restoration, only the distribution at the top surface of the cement layer was evaluated.

When the crown was perfectly bonded (Stage 1), the maximum tensile stress at the top surface of cement layer was approximately 14 MPa, and the stress distribution was quite uniform. Once debonding occurred, a stress concentration developed at the edge of the debond front as evident in (Figs. 5(b)-(g)) and the magnitude of stress increased with the extent of debonding. The largest tensile stress, which developed in Stage 5, exceeded the flexural strength (127 MPa) of the luting cement [49].

The stress distribution at the top surface of the cement layer caused by interfacial defects is shown in Figs. 5(h) and 5(i). Stress concentrations appeared along the boundary of the defects. Furthermore, the stress concentration was more severe than that in uniform debonding, except for Stage 5. In the two cases of distributed defects, the magnitude of stress in Case II exceeded that of Case I, which was consistent with the stresses in the crown.

3.2 Failure risk

The average stress ($\bar{\sigma}$) is estimated according to Eq. (3) at the internal surface of the monilithic crown and is presented as a function of the debonded area in Fig. 6. It is evident that the average stress increased with debonding from Stage 1 to 5. Thus, debonding along the inner wall of the crown increases the average stress in the crown, which is detrimental to

the durability of the restoration. From Stage 5 to 7, the average stress reached a plateau.

The maximum tensile stress and the average stress were also evaluated for each of the seven stages of debonding and the two cases of interfacial defects in the luting process. These values are shown in Figs. 7 and 8, respectively. Note that the results are plotted according to the degree of separation at the interface. As evident from Fig.7, all the maximum tensile stress values were lower than the flexural strength (about 400 MPa) of the lithium disilicate IPS e.max CAD [50], which indicates the internal surface of the crown is safe to sustain the 600 N vertical load. It was also found that the maximum tensile stress was greatest for the interfacial defects of Case II, although the average stress was lower for this condition.

Besides, the comprehensive risk of failure of the monolithic crown (κ) was analyzed accordingly to Eq. (4) and results are shown in Fig. 9. Interestingly, Case II and Stage 5 were the most severe. Although the separation area caused by the interfacial defects was only 13% for Case II and far less than that in Stage 2 of debonding, the stress concentration in the crown was much greater.

For the cement, the concept of percent damage is introduced, which is the ratio of the area in which the maximum principal stress is greater than or equal to the ultimate tensile strength (flexural strength 127 MPa for the Rely X ARC [49]) of the material, over the total area at the interface. This concept is used to assess the degree of risk of cement failure for the various conditions (Fig. 10). Similar to Fig. 9, Case II of interfacial defects, and Stage 5 of debonding are most severe of the conditions analyzed.

4. Discussion

The vertical concentrated load applied through the rigid hemisphere at the center of the restored crown resulted in three contact zones on the occlusal surface. Dental ceramics are brittle materials and undergo failure as a result of the magnitude of the first principle stress. They are sensitive to defects that cause a concentration of tensile stress in the case of a crack. Hence, the maximum principal stress within the crown was evaluated. Although the maximum tensile stress (about 450 MPa) at the three contact zones exceeded the reported flexural strength (about 400 MPa) of IPS e.max [50], these three locations were disregarded since the areas of contact in the mouth are large, thereby causing reduction in tensile stress in the occlusal surface. In addition, the stress between the cement and substrate is less than that on top surface of the cement. Because the elastic modulus of the substrate is less than that of the crown and Poisson's ratio is larger than that of the crown, according to the elastic theory, the allocation of external occlusal force at the interface between crown and cement will be larger than that at the interface between substrate and cement. That is justified focusing on the stress distribution on the internal surface of the crown and the top surface of the cement.

Clelland et al. [51] reported that the quality of bonding influenced the long-term survival of glass-ceramics after a specific duration of service. Combined with the response in Fig. 6, this suggests that the integrity of the interface is a contributing factor in the survival rates of bonded restorations. Debonding often initiates at the margin of the restoration and extends along the interface towards the occlusal region [36]. This evolution of debonding was described by the seven-stage process.

Although the separation area caused by the interfacial defects was only 13% for Case II which was far less than that in Stage 2 of debonding, the stress concentration as well as the

failure risk in this case was much severe, which indicates that the defects introduced in luting process are more detrimental on integrity of the ceramic restoration than that of debonding. This signifies that the integrity of the luting process is very important for maintaining the monolithic crown intact. It is important to recognize the significance of the finding in Fig. 9. Debonding and interfacial defects increase the failure risk of stress-based by up to 700% with respect to the perfectly bonded condition (stage 1). As a consequence, the null hypothesis must be rejected. For contemporary dental adhesives, the fundamental principle of adhesion to tooth substrate is based upon an exchange process by which inorganic tooth material is exchanged for synthetic resin [52]. It is reported that resin cement may fill the defects like voids and microcracks existing in the ceramic [53, 54]. Kenneth et al. also reported that acid-etched Dicor restorations luted with resin composite exhibited more favorable survivor functions than restorations luted with glass ionomer or zinc phosphate agents [55]. So, the resin cement would be better than the glass ionomer or zinc phosphate to obtain durability for the restorations.

In previous finite element studies focused on the fracture of ceramic restorative systems, simplified crowns have been defined with ideal multi-layer structure and perfectly bonded interfaces [e.g. 56-58]. In general, the applied concentrated load required for fracture is fairly large, while in clinical applications fractured crowns occur at the magnitude of loads encountered during mastication. Results from the present study provide a partial explanation for this discrepancy. Degradation of the bonded interface and micro defects resulting from the luting process may play an important role in maintaining the restoration strength.

From Fig. 4 and Fig. 5, it was found that the stress in the wall of the crown increases

with debonding as it progresses from the margin, which indicates that the axial wall of the ceramic crown acts as a ferrule [33] to fix the restoration on top of the tooth substrate in the completely bonding situation. It also plays a critical role in maintaining the principal tensile stress of the crown at an acceptable level. Hence, simplifying the crown to a plate or disk without considering the axial wall [32, 59, 60] is a conservative evaluation of the restorations. Besides, since the axial wall does not directly carry the occlusal load, the thickness decreases towards the margin, moreover, the stress in the wall increases with debonding as it progresses from the margin, which may facilitate crack initiation and growth from defects in the ceramic, and eventually lead to fracture of the restoration. This prediction is in good agreement with the case studies for all-ceramic crowns that most failures did not initiate from the contact surface, but at the resin cement interface [61] or the margin areas of the crown [15].

In addition, the failure risk κ proposed in present study is a straightforward quantity to estimate the durability of the ceramic crowns. For a structure composed of brittle materials, the fatigue life depends on the stress level. The higher the stress level is, the shorter the fatigue life will be. However, stress level not only relies on the average stress $\bar{\sigma}$, but also depends on the maximum tensile stress σ_{max}. According to the fatigue theory [62], the stress level is positively correlated with $\bar{\sigma}$ and σ_{max}. Moreover, According to Corten-Dolan's cumulative damage model [63-65], fatigue damage $\boldsymbol{D}$ after N cycles of fatigue load is estimated by the following equation

$$D = mrN^{a} \tag{5}$$

where m is the number of damage nuclei, which is positively correlated with the stress level; r is coefficient of damage propagation rate depending on stress level, which is directly

proportional to the stress level; a is a constant. The failure risk κ is positively related with the the product $\bar{\sigma} \times \sigma_{max}$, which indicates that κ increases with fatigue damage $\boldsymbol{D}$.

In this investigation, the influence of bond quality and degree of debonding on the stress distribution within a monolithic lithium disilicate crown were evaluated. It is generally accepted that the durability of the crown and its resistance to fracture increase with bond quality [66]. Two factors that can reduce the bond quality were considered herein, including microscopic defects in the luting cement and progressive debonding of the cement from the crown. In the clinic environment, the root cause of fracture is often considered to be the result of a single mechanism. Similarly, previous numerical studies of the stress distribution in crowns considered cement conditions involving either perfectly bonded or completely debonded [45, 48, 57, 67]. The variation of stress caused by imperfect interfaces and the corresponding localized stress concentration within the crown were not considered. Admittedly, it is difficult to identify the fracture mechanisms contributing to crown failures using the FEA method [45]. However, by utilizing a multi-stage debonding process, and considering discrete cases of distributed microscopic defects, the evolution of stress in the crown and cement layer was elucidated under a constant occlusal force. In addition, by introducing a risk of failure concept (κ) that accounts for both defects in the luting cement and degradation of the interface with the evolution of oral function, results of the numerical simulation describe the relative increase in risk of failure caused by imperfect bonding. With an increased risk of crown failure of up to 700% over that with perfect bonding, the results further establish the importance of improving the adhesive and bond integrity towards maximizing the durability of all-ceramic crowns.

Apart from the clinical significance of the findings, there are some limitations to the investigation that warrant discussion. For instance, only debonding at the interface between the crown and cement was considered, as would arise from cyclic stress or moisture. However, the other effects of moisture were neglected. Lu et al. [36] reported that there is a reduction in Young's modulus of the cement and overall loss of bond strength. However, due to the substantial different in elastic modulus between crown and cement, there is minimal change in the stress distribution with reduction in Young's modulus of the cement. Furthermore, only vertical occlusal loading was considered in the simulations. Duan et al. [68] demonstrated that the distribution of stress in crowns was not dependent on the bite force, but the maximum stress could increase with the introduction of a lateral component of loading. That would increase the detrimental effects of interfacial defects. Therefore, the interfacial stresses and estimated risks of failure reported here could be conservative.

The interface between the crown and cement was the primary focus as it is highly dependent on the clinical preparation and luting process. However, the interface between tooth abutment and cement can be influenced by many factors as well, including the presence of dentinal fluid, intratubular pressure and permeability of the dentin [69]. Additionally, water sorption occurs within the cement and is both time and thickness dependent [28]. As such, water is not a controllable variable [28], especially at the interface between substrate and cement. Consequently, the interface between crown and cement was of interest to be evaluated. Perfect bonding between cement and substrate was assumed in the present study as a simplification for the uncontrolled moisture and its potential contribution to degradation. It is conceivable that the maximum stress in the crown under the same load conditions would

be more severe clinically than that of the ideal FEA model. Clearly, additional work addressing this topic is warranted.

5. Conclusion

Within the limitations of the results, the following conclusions have been drawn:

(1) The average principal tensile stress (i.e. average stress, $\overline{\sigma}$) reduces the durability of brittle materials subjected to cyclic stress, and that failure of a brittle material is a function of both $\overline{\sigma}$ and σ_{max}.

(2) For the monolithic lithium disilicate CAD/CAM crowns, the risk of crown failure risk is not only associated with the area of debonding at the cement/crown interface, but also associated with the distribution of debonding.

(3) Defects in the bonded interface are more detrimental to the crown durability than simply uniform interfacial debonding, and surprisingly, potentially more critical than a completely debonded interface. Avoiding the defects within the interface between crown and cement is a key requirement to improving the durability of ceramic restorations.

(4) This paper demonstrated that adhesive bonding along the axial wall plays a critical role in maintaining the average principal tensile stress of the crown at an acceptable level. Flat plate or disc models for crowns lead to conservative estimates in comparison to the actual crown.

Acknowledgments

The authors would like to thank the National Natural Science Foundation of China through grants #11672347, #51732008 and # 11727804. The financial support from the National Natural Science Foundation of Shanghai through grants #14ZR1432700 is also gratefully acknowledged.

References

[1] A.R. Studart, F. Filser, P. Kocher, H. Lüthy, L. J. Gauckler, Mechanical and fracture behavior of veneer–framework composites for all-ceramic dental bridges, Dent. Mater. 23 (2007) 115-123.

[2] H. Fischer, G. Dautzenberg, R. Marx, Nondestructive estimation of the strength of dental ceramic materials, Dent. Mater. 17 (2001) 289-295.

[3] A. Imanishi, T. Nakamura, T. Ohyama, 3-D Finite element analysis of all-ceramic posterior crowns, J. Oral. Rehabil. 30 (2003) 818-822.

[4] W. Yu, K. Guo, B. Zhang, W. Weng, Fracture resistance of endodontically treated premolars restored with lithium disilicate CAD/CAM crowns or onlays and luted with two luting agents, Dent. Mater. J. 33 (2014) 349-354.

[5] S. Kitayama, P. Pilecki, N.A. Nasser, T. Bravis, R.F. Wilson, T. Nikaido, J. Tagami, T.F. Waston, R.M. Foxton, Effect of resin coating on adhesion and microleakage of computer‐aided design/computer‐aided manufacturing fabricated all‐ceramic crowns after occlusal loading: a laboratory study, Eur. J. Oral. Sci. 117 (2009) 454-462.

[6] C.J. Ho, H.C. Liu, W.H. Tuan, Effect of abrasive grinding on the strength of Y-TZP, J. Eur.

Ceram. Soc. 29(2009) 2665-2669.

[7] M. Subash, D. Vijitha, S. Deb, A. Satish, N. Mahendirakumar, Evaluation of shear bond strength between zirconia core and ceramic veneers fabricated by pressing and layering techniques: In vitro study, J. Pharm. Pract. 7 (Suppl 2) (2015) S6 12-15.

[8] T.A. Sulaiman, A.A. Abdulmajeed, K. Shahramian, L. Lassila, Effect of different treatments on the flexural strength of fully versus partially stabilized monolithic zirconia, J. Prosthet. Dent. 118 (2017) 216-220.

[9] M. Al-Akhali, M.S. Chaar, A. Elsayed, A. Samran, M. Kern, Fracture resistance of ceramic and polymer-based occlusal veneer restorations, J. Mech. Behav. Biomed. Mater. 74 (2017) 245-250.

[10] H. ÖZDEMİR, A. ÖZDOĞAN, The effect of heat treatments applied to superstructure porcelain on the mechanical properties and microstructure of lithium disilicate glass ceramics, Dent. Mater. J (2017) 1-9.

[11] G. Tysowsky, The science behind lithium disilicate: today's surprisingly versatile, esthetic & durable metal-free alternative, Oral. Health. J. 23 (2009) 93-97.

[12] D.J. Fasbinder, J.B. Dennison, D. Heys, G. Neiva, A clinical evaluation of chairside lithium disilicate CAD/CAM crowns, J. Am. Dent. Assoc. 141 (2010) 10S-14S.

[13] P.C. Guess, R.A. Zavanelli, N.R. Silva, E.A. Bonfante, P.G. Coelho, V.P. Thompson, Monolithic CAD/CAM lithium disilicate versus veneered Y-TZP crowns: comparison of failure modes and reliability after fatigue, Int. J. Prosthodont, 23 (2010) 434-442.

[14] N.R.F.A. Silva, E.A. Bonfante, L.M. Martins, G.B. Valverde, V.P. Thompson, J.L. Ferencz, P.G. Coelho, Reliability of reduced-thickness and thinly veneered lithium

disilicate crowns, J. Dent. Res. 91 (2012) 305-310.

[15] S. Nasrin, N. Katsube, R.R. Seghi, S.I. Rokhlin, Survival Predictions of Ceramic Crowns Using Statistical Fracture Mechanics, J. Dent. Res. 96 (2017) 509-515.

[16] S.R. Ha, S.H. Kim, J.B Lee, J.S. Han, I.S. Yeo, S.H. Yoo, H.K. Kim, Biomechanical three-dimensional finite element analysis of monolithic zirconia crown with different cement thickness, Cearm. Int. 42 (2016) 14928-14936.

[17] Y. Jian, Z.H. He, L. Dao, M.V. Swain, X.P. Zhang, K. Zhao, Three-dimensional characterization and distribution of fabrication defects in bilayered lithium disilicate glass-ceramic molar crowns, Dent. Mater. 33 (2017) e178-185.

[18] M.N. Aboushelib, A.J. Feilzer, C.J. Kleverlaan, Bridging the gap between clinical failure and laboratory fracture strength tests using a fractographic approach, Dent. Mater. 25 (2009) 383-391.

[19] Z. Zhang, S. Zhou, Q. Li, W. Li, M.V. Swain, Sensitivity analysis of bi-layered ceramic dental restorations, Dent. Mater. 28 (2012) e6-14.

[20] U. Lohbauer, R. Belli, G. Arnetzl, S.S. Scherrer, G.D. Quinn, Fracture of a veneered-ZrO 2 dental prosthesis from an inner thermal crack, Case. Stud. Eng. Fail. Anal. 2 (2014) 100-106.

[21] J.Y. Thompson, K.J. Anusavice, A. Naman, H.F. Morris, Fracture surface characterization of clinically failed all-ceramic crowns, J. Dent. Res. 73 (1994) 1824-1832.

[22] R. Danzer, T. Lube, P. Supancic, R. Damani, Fracture of ceramics, Adv. Eng. Mater. 10 (2010) 275-298.

[23] K. Zhao, Y. Pan, P.C. Guess, X. P. Zhang, M.V. Swain, Influence of veneer application on fracture behavior of lithium-disilicate-based ceramic crowns, Dent. Mater. 28 (2012) 653-660.

[24] M. Ozcan, PK. Vallittu, Effect of surface conditioning methods on the bond strength of luting cements to ceramics, Dent. Mater. 19 (2003) 725–731.

[25] H.R. Horn, Porcelain laminate veneers bonded to etched enamel, Dent. Clin. North. Am. 27 (1983) 671–84.

[26] DM. Wolf, JM. Powers, KL. O'Keefe, Bond strength of composite to etched and sandblasted porcelain, Am. J. Dent. 6 (1993) 155–158.

[27] J.P. Matinlinna, L.V. Lassila, M. Ozcan, A. Yli-Urpo, P.K. Vallitu, An introduction to silanes and their clinical applications in dentistry, Int. J. Prosthodont.17 (2004) 155–164.

[28] L.G. May, J.R. Kelly, M.A. Bottino, T. Hill, Effects of cement thickness and bonding on the failure loads of CAD/CAM ceramic crowns: multi-physics FEA modeling and monotonic testing, Dent. Mater. 28 (2012) e99-109.

[29] N. Manuja, R. Nagpal, I.K. Pandit, Dental adhesion: mechanism, techniques and durability, J. Clin. Pediatr. Dent. 36 (2012) 223-234.

[30] M.J. Lim, K.W. Lee, Effect of adhesive luting on the fracture resistance of zirconia compared to that of composite resin and lithium disilicate glass ceramic, Restor. Dent. Endod. 42 (2017) 1-8.

[31] F. Alqahtani, Marginal fit of all-ceramic crowns fabricated using two extraoral CAD/CAM systems in comparison with the conventional technique, Clin. Cosmet. Investig. Dent. 9 (2017) 13-18.

[32] R.P. Pagniano, R.R. Seghi, S.F. Rosenstiel, R. Wang, N. Katsube, The effect of a layer of resin luting agent on the biaxial flexure strength of two all-ceramic systems, J. Prosthet. Dent. 93 (2005) 459-466.

[33] M.M. Gresnigt, M. Özcan, M.L. van den Houten, L. Schipper, M.S. Cune, Fracture strength, failure type and Weibull characteristics of lithium disilicate and multiphase resin composite endocrowns under axial and lateral forces, Dent. Mater. 32 (2016) 607-614.

[34] S.M. Marocho, M. Ozcan, R. Amaral, M.A. Bottino, L.F. Valandro, Effect of resin cement type on the microtensile bond strength to lithium disilicate ceramic and dentin using different test assemblies, J. Adhes. Dent. 15(2013) 361-368.

[35] M.M. Aboumadina, M. Özcan, K.M. Abdelaziz, Influence of resin cements and aging on the fracture resistance of IPS e.max press posterior crowns, Int. J. Prosthodont. 25 (2012) 33-35.

[36] C. Lu, R. Wang, S. Mao, D. Arola, D. Zhang, Reduction of load-bearing capacity of all-ceramic crowns due to cement aging, J. Mech. Behav. Biomed. Mater. 17 (2013) 56-65.

[37] H. Lekesiz, Reliability estimation for single-unit ceramic crown restorations, J. Dent. Res. 93 (2014) 923-928.

[38] A. Piwowarczyk, H.C. Lauer, J.A. Sorensen, Microleakage of various cementing agents for full cast crowns, Dent. Mater. 21 (2005) 445-453.

[39] A.I. Hernandez, T. Roongruangphol, N. Katsube, R.R. Seghi, Residual interface tensile strength of ceramic bonded to dentin after cyclic loading and aging, J. Prosthet. Dent. 99 (2008), 209-217.

[40] D. Cortellini, A. Canale, Bonding lithium disilicate ceramic to feather-edge tooth preparations: a minimally invasive treatment concept, J. Adhes. Dent. 14 (2012) 7-10.

[41] M. Gehrt, S. Wolfart, N. Rafai, S. Reich, D. Edelhoff, Clinical results of lithium disilicate crowns after up to 9 years of service, Clin. Oral. Investig. 17 (2013) 275-284.

[42] S. Reich, O. Schierz, Chair-side generated posterior lithium disilicate crowns after 4 years, Clin. Oral. Investig. 17 (2013) 1765-1772.

[43] M.A. Carvalho, B. S. Sotto-Maior, A.A.D.B. Cury, G.E.P. Henriques, Effect of platform connection and abutment material on stress distribution in single anterior implant-supported restorations: A nonlinear 3-dimensional finite element analysis, J. Prosthet. Dent. 112 (2014) 1096-1102.

[44] N. Emami, K.J.M. Söderholm, L.A. Berglund, Effect of light power density variations on bulk curing properties of dental composites, J. Dent. 31 (2003) 189-196.

[45] R.E. Campos, P.V. Soares, A. Versluis, O.B.D.O. Júnior, G.M. Ambrosano, I.F. Nunes, Crown fracture: Failure load, stress distribution, and fractographic analysis, J. Prosthet. Dent. 114 (2015) 447-455.

[46] C. F. Han, B.H. Wu, C.J. Chung, S.F. Chuang, W.L. Li, J.F. Lin, Stress-strain analysis for evaluating the effect of the orientation of dentin tubules on their mechanical properties and deformation behavior, J. Mech. Behav. Biomed. Mater. 12 (2012) 1-8.

[47] X. Wu, M. Nakagawa, F. Teraoka, Failure morphology of all-ceramic prostheses, Dent. Mater. J. 31 (2012) 494-498.

[48] P.G. Coelho, E.A. Bonfante, N.R.F. Silva, E.D. Rekow, V.P. Thompson, Laboratory simulation of Y-TZP all-ceramic crown clinical failures, J. Dent. Res. 88(2009) 382-386.

[49] T.R. Aguiar, M. De Oliveira, C.A. Arrais, G.M. Ambrosano, F. Rueggeberg, M. Giannini, The effect of photopolymerization on the degree of conversion, polymerization kinetic, biaxial flexure strength, and modulus of self-adhesive resin cements, J. Prosthet. Dent. 113 (2015) 128-134.

[50] S.H. Kang, J. Chang, S. Ho-Hyun, Flexural strength and microstructure of two lithium disilicate glass ceramics for CAD/CAM restoration in the dental clinic, Restor. Dent. Endod. 38 (2013) 134-140.

[51] N.L. Clelland, A. Ramirez, N. Katsube, R.R. Seghi, Influence of bond quality on failure load of leucite- and lithia disilicate- based ceramics, J. Prosthet. Dent. 97 (2007) 18-24.

[52] B. Van Meerbeek, M. Vargas, S. Inoue, Y. Yoshida, M. Peumans, P. Lambrechts, G. Vanherle, Adhesives and cements to promote preservation dentistry, Oper. Dent. Suppl 6 (2001)119-144.

[53] G. J. Fleming, G. Bhamra, P.M. Marquis,The strengthening mechanism of resin cements on porcelain surfaces, J. Dent. Res. 85 (2006) 272-276.

[54] P. Marquis, The influence of cements on the mechanical performance of dental ceramics, Bioceram. 5 (1992) 317-324.

[55] K.A. Malament, S.S. Socransky, Survival of dicor glass-ceramic dental restorations over 16 years. part III: effect of luting agent and tooth or tooth-substitute core structure, J. Prosthet. Dent. 86 (2001) 511-519.

[56] Y. Zhang, J.J.W. Lee, R. Srikanth, B.R. Lawn, Edge chipping and flexural resistance of monolithic ceramics, Dent. Mater. 29 (2013) 1201-1208.

[57] Y. Deng, P. Miranda, A. Pajares, F. Guiberteau, B.R. Lawn, Fracture of

ceramic/ceramic/polymer trilayers for biomechanical applications, J. Biomed. Mater. Res. (Part A) 67 (2003) 828-833.

[58] H. Chai, B. Lawn, S. Wuttiphan, Fracture modes in brittle coatings with large interlayer modulus mismatch, J. Mater. Res. 14 (1999) 3805-3817.

[59] Y. Zhang, B.R. Lawn, K.A. Malament, T.P. Van, E.D. Rekow, Damage accumulation and fatigue life of particle-abraded ceramics, Int. J. Prosthodont. 19 (2006) 442-448.

[60] Y. Zhang, J.W. Kim, S. Bhowmick, V.P. Thompson, E.D. Rekow, Competition of fracture mechanisms in monolithic dental ceramics: flat model systems, J. Biomed. Mater. Res. B. Appl. Biomater. 88 (2009) 402–411.

[61] S. Nasrin, N. Katsube, R.R. Seghi, S.I. Rokhlin, 3D statistical failure analysis of monolithic dental ceramic crowns, J. Biomech. 49 (2016) 2038-2046.

[62] J. Schijve, Fatigue of structures and materials, Springer, New York, 2008.

[63] H. Gao, H.Z. Huang, Z. Lv, F.J. Zuo, H.K. Wang, An improved corten-dolan's model based on damage and stress state effects, J. Mech. Sci. Technol. 29 (2015) 3215-3223.

[64] S.P. Zhu, H.Z. Huang, Yu. Liu, L.P. He, Q. Liao, A practical method for determining the corten-dolan exponent and its application to fatigue life prediction, Int. J. Turbo. Jet. Eng. 29 (2012) 79-87.

[65] H.T. Corten, T.J. Dolon, Cumulative fatigue damage, Proceedings of the International Conference on Fatigue of Metals. (1956) 235-246.

[66] R.V. Kumari, R.K. Poluri, H. Nagaraj, K. Siddaruju, Comparative Evaluation of Bond Strength of Dual-Cured Resin Cements: An In-Vitro Study, J. Int. Oral. Health. 7 (Suppl 1) (2015) 43-47.

[67] C. González-Lluch, A. Pérez-González, Analysis of the effect of design parameters and their interactions on the strength of dental restorations with endodontic posts, using finite element models and statistical analysis, Comput. Methods. Biomech. Biomed. Engin. 19 (2015) 428-439.

[68] Y. Duan, J.A. Griggs, Effect of elasticity on stress distribution in CAD/CAM dental crowns: glass ceramic vs. polymer-matrix composite, J. Dent. 43 (2015) 742-749.

[69] G.C. Lopes, L.N. Baratieri, M.A. de Andrada, L.C. Vieira, Dental adhesion: present state of the art and future perspectives, Quintessence. Int. 33 (2002) 213-224.

Table 1 - Material properties and numbers of elements and nodes in the FEA models. The properties are from the studies of [36, 43, 44].

Material	Elastic Modulus (GPa)	Poisson's ratio	Number of elements	Number of nodes
Lithium disilicate (Crown)	*96.0*	*0.23*	*226562*	*84964*
Rely X ARC (cement)	*6.5*	*0.27*	*650337*	*172363*
Tooth substrate	*12.9*	*0. 30*	*244023*	*84856*

List of Figures

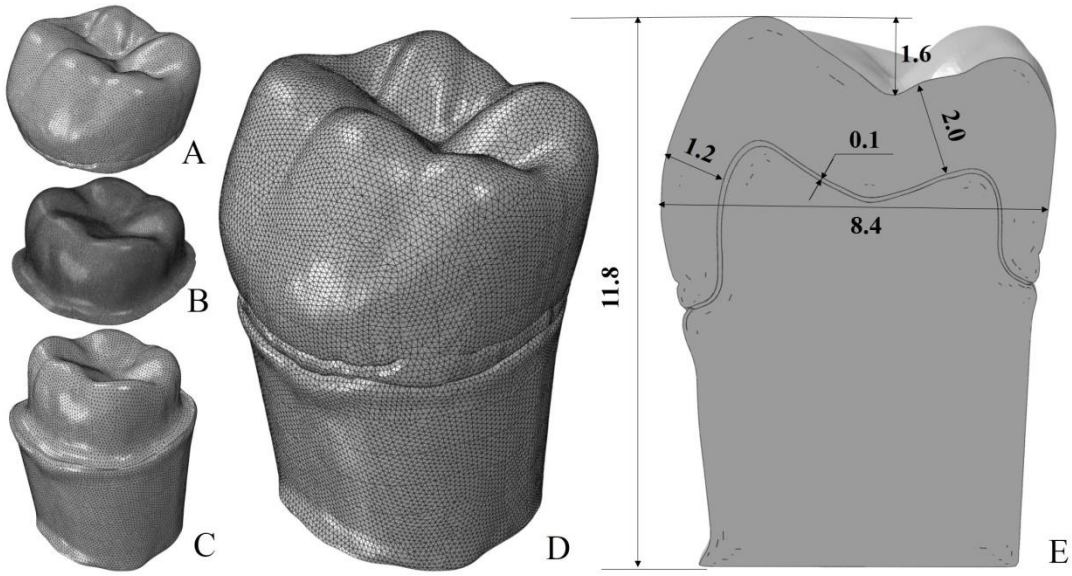

Fig. 1 - The numerical model of the monolithic restoration. (A) crown; (B) cement layer; (C) tooth abutment; (D) meshed model; (E) relative dimensions of the model (mm).

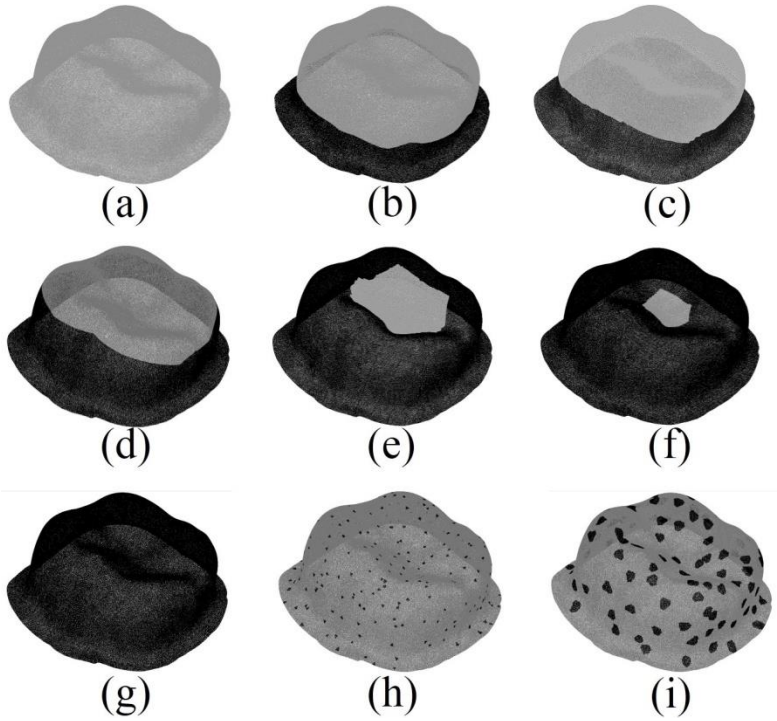

Fig.2 - Definitions for the interface debonding and randomly distributed defects. The seven stages of debonding correspond to a) I: 0%, b) II: 29%, c) III: 38%, d) IV: 59%, e) V: 75%, f) VI: 87% and g) VII: 100%. Randomly distributed defects were considered with h) Case I: 130 μm average nominal diameter and 2.6% distribution and i) Case II: 500 μm average nominal diameter and 13.3% distribution.

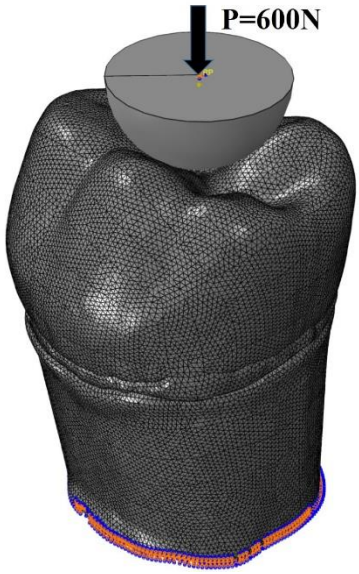

Fig. 3 - Occlusal loading condition through rigid hemisphere with diameter of 5 mm.

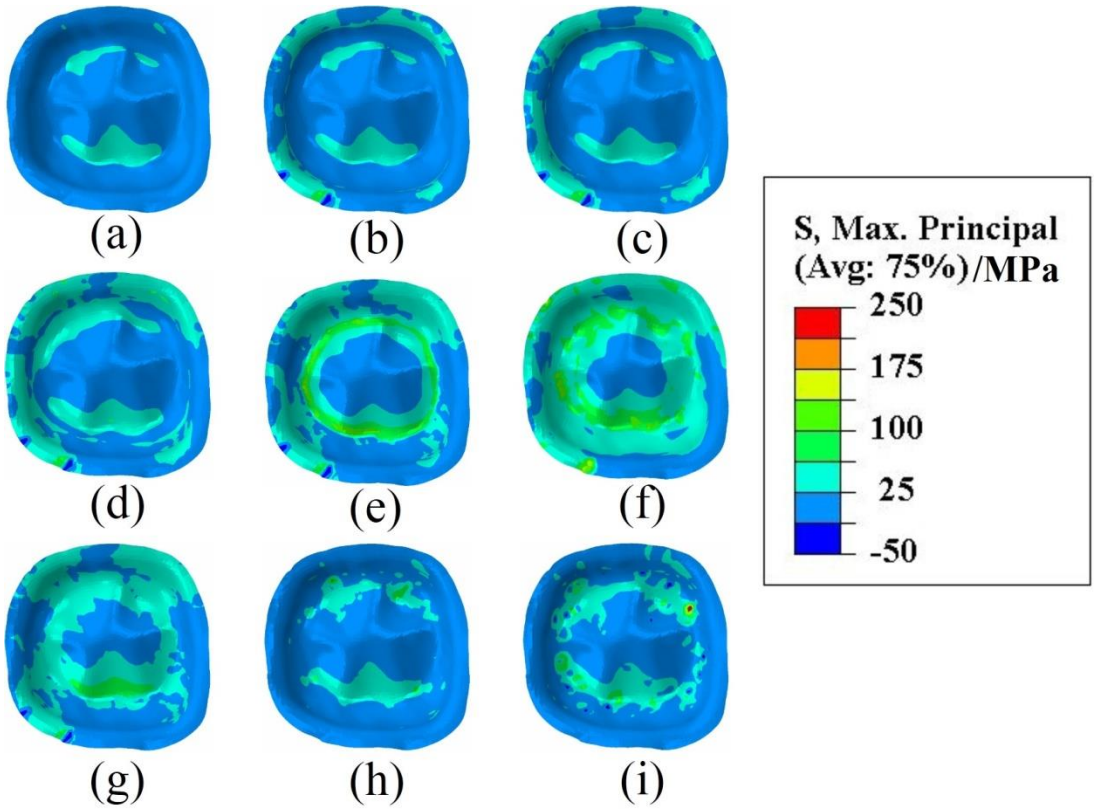

Fig. 4 - Stress distributions at the internal surface of the monolithic crown corresponding to the seven stages of debonding ((a) – (g)) and the two cases of interfacial defects ((h),(i)).

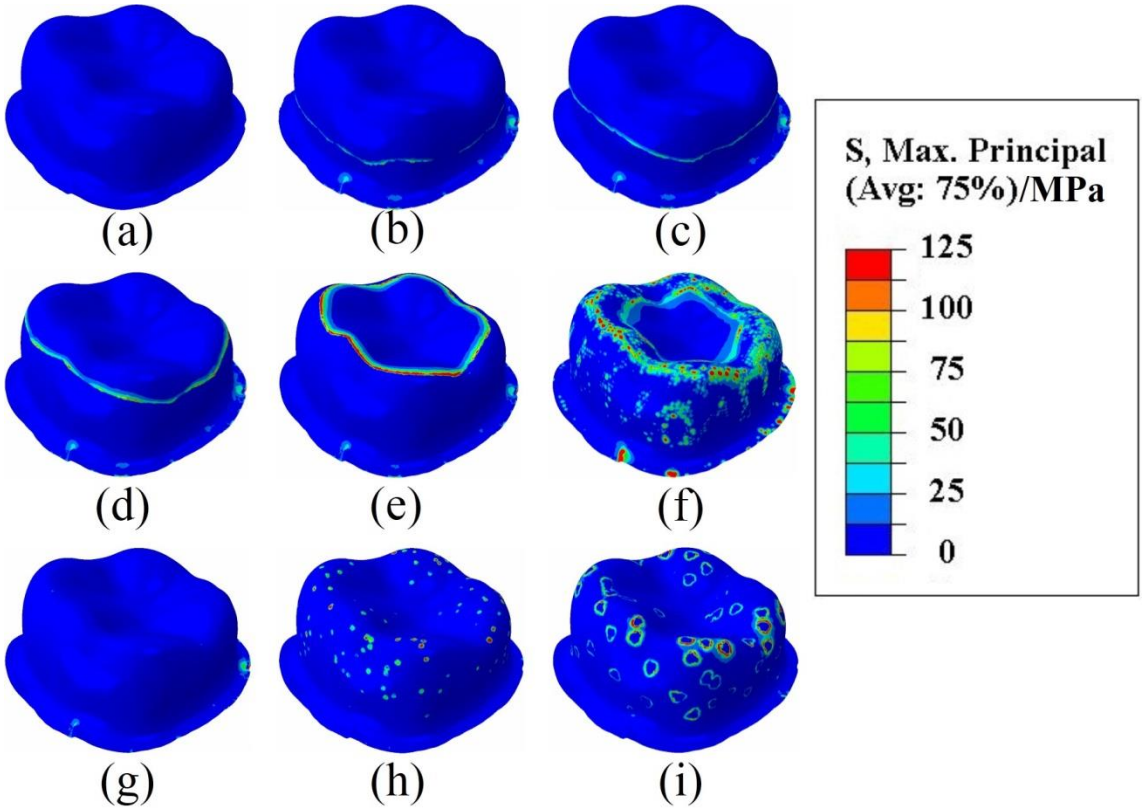

Fig. 5 - Stress distribution at the top surface of the cement layer corresponding to the seven stages of debonding ((a) – (g)) and the two cases of interfacial defects ((h), (i)).

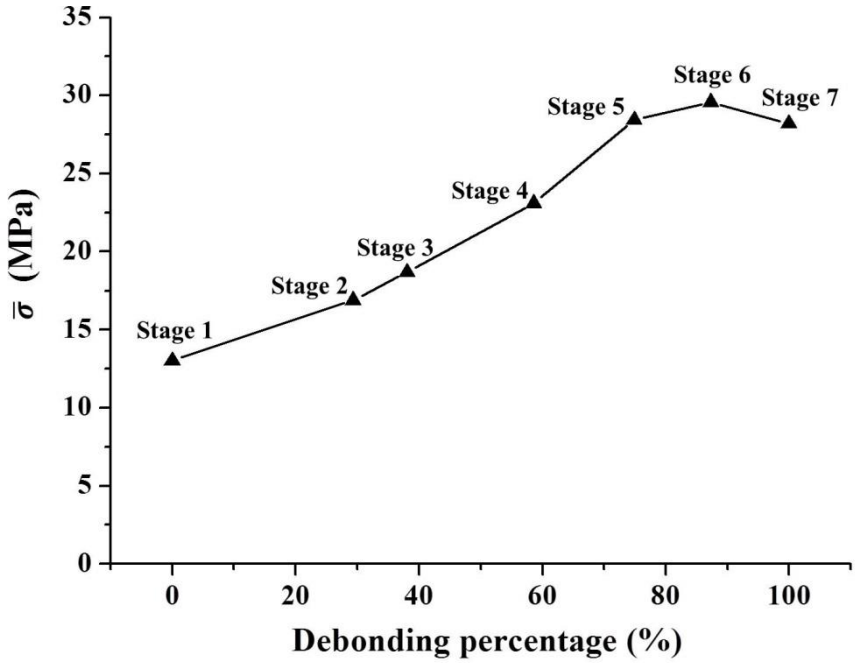

Fig. 6 - The average stress along the interior surface as a function of the seven stages of debonding.

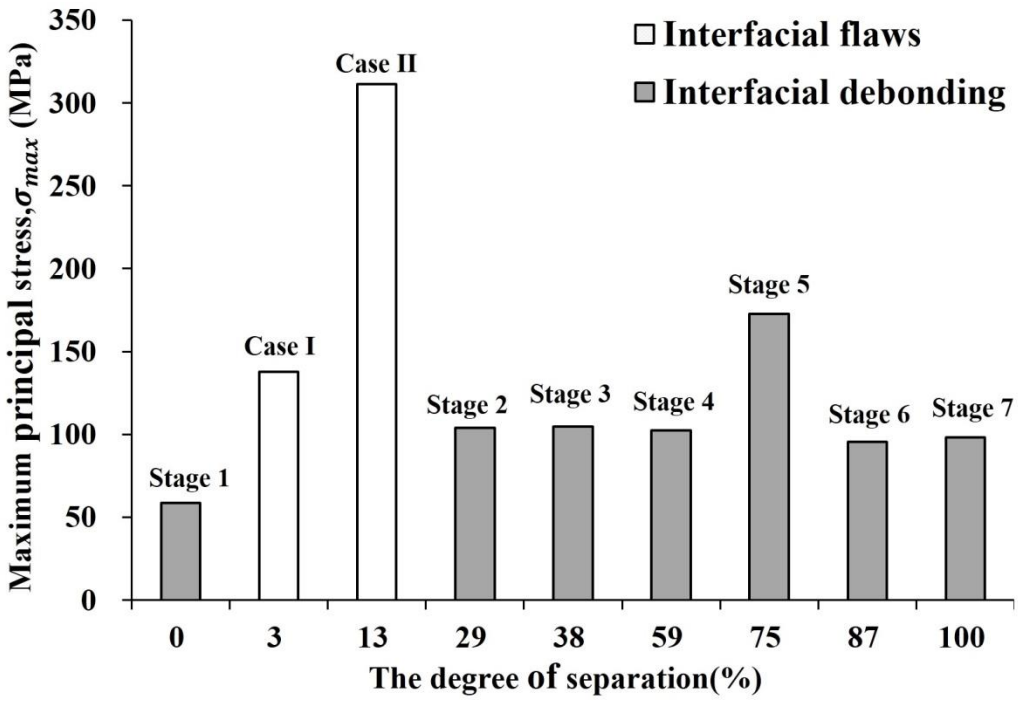

Fig. 7 - The maximum values of principal stress in the crown in terms of the degree of separation between the crown and cement.

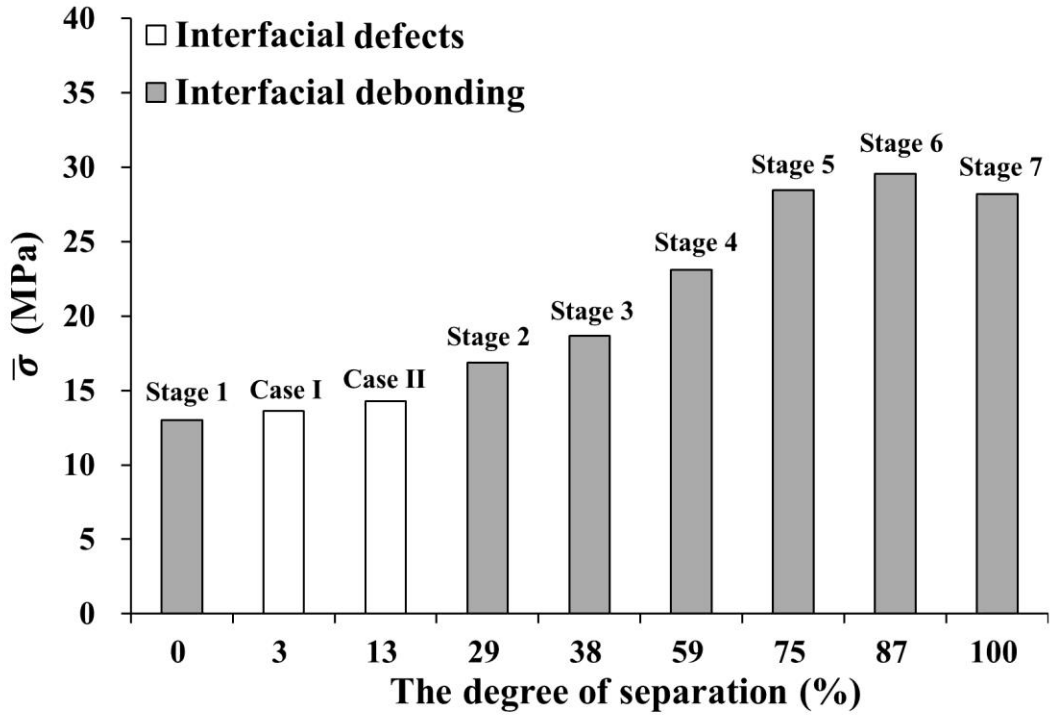

Fig. 8 - The average stress in terms of the degree of separation between the cement and crown.

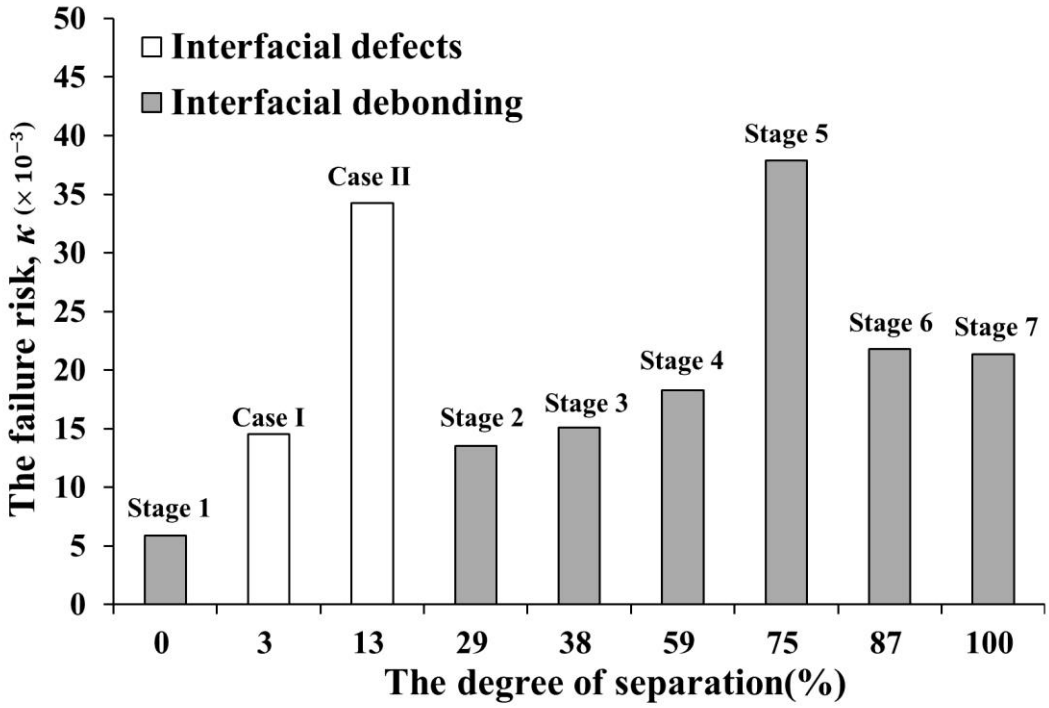

Fig. 9 - The failure risk κ in terms of the degree of separation.

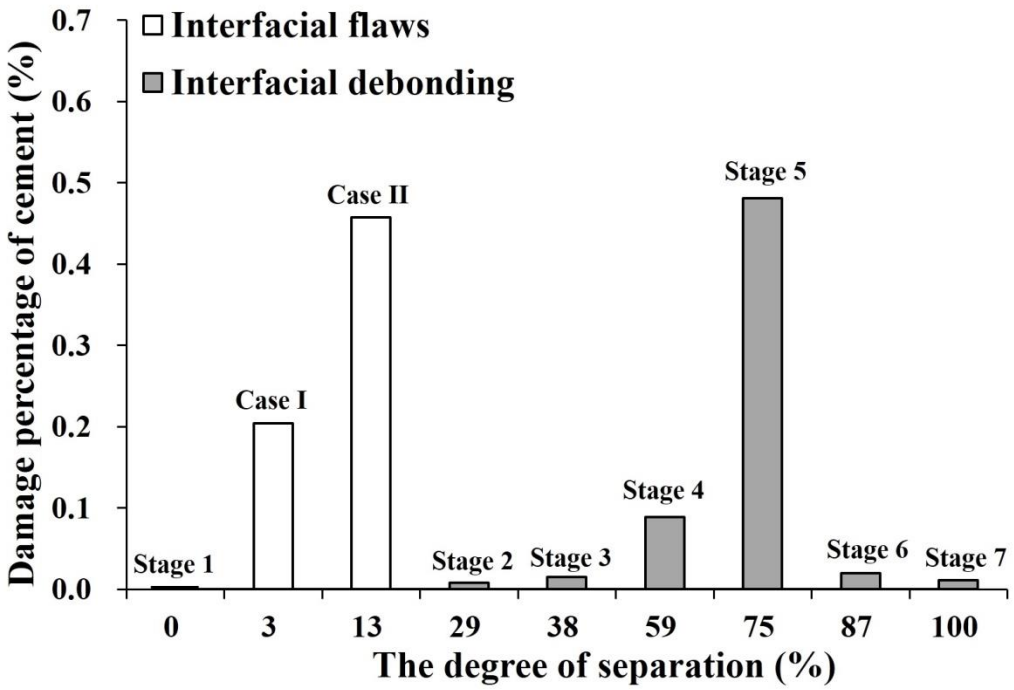

Fig.10 - Damage percentage within the cement layer for interfacial debonding and for interfacial defects in terms of the degree of separation.